NASA/TM–20230010640
NESC-RP-21-01718

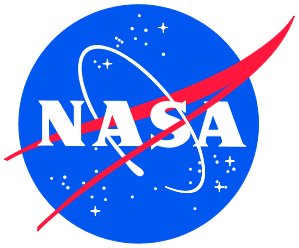

Space-Shielding Radiation Dosage Code Evaluation

Phase 1: SHIELDOSE-2 Radiation-Assessment Code

Steven J. Gentz/NESC
Langley Research Center, Hampton, Virginia

Insoo Jun
Jet Propulsion Laboratory, Pasadena, California

July 2023

NASA STI Program Report Series

Since its founding, NASA has been dedicated to the advancement of aeronautics and space science. The NASA scientific and technical information (STI) program plays a key part in helping NASA maintain this important role.

The NASA STI program operates under the auspices of the Agency Chief Information Officer. It collects, organizes, provides for archiving, and disseminates NASA's STI. The NASA STI program provides access to the NTRS Registered and its public interface, the NASA Technical Reports Server, thus providing one of the largest collections of aeronautical and space science STI in the world. Results are published in both non-NASA channels and by NASA in the NASA STI Report Series, which includes the following report types:

- TECHNICAL PUBLICATION. Reports of completed research or a major significant phase of research that present the results of NASA Programs and include extensive data or theoretical analysis. Includes compilations of significant scientific and technical data and information deemed to be of continuing reference value. NASA counterpart of peer-reviewed formal professional papers but has less stringent limitations on manuscript length and extent of graphic presentations.

- TECHNICAL MEMORANDUM. Scientific and technical findings that are preliminary or of specialized interest, e.g., quick release reports, working papers, and bibliographies that contain minimal annotation. Does not contain extensive analysis.

- CONTRACTOR REPORT. Scientific and technical findings by NASA-sponsored contractors and grantees.

- CONFERENCE PUBLICATION. Collected papers from scientific and technical conferences, symposia, seminars, or other meetings sponsored or co-sponsored by NASA.

- SPECIAL PUBLICATION. Scientific, technical, or historical information from NASA programs, projects, and missions, often concerned with subjects having substantial public interest.

- TECHNICAL TRANSLATION. English-language translations of foreign scientific and technical material pertinent to NASA's mission.

Specialized services also include organizing and publishing research results, distributing specialized research announcements and feeds, providing information desk and personal search support, and enabling data exchange services.

For more information about the NASA STI program, see the following:

- Access the NASA STI program home page at http://www.sti.nasa.gov

- Help desk contact information:

https://www.sti.nasa.gov/sti-contact-form/
and select the "General" help request type.

NASA/TM–20230010640
NESC-RP-21-01718

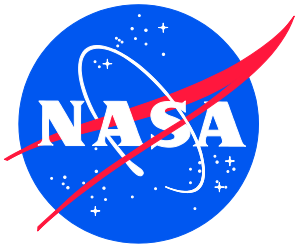

Space-Shielding Radiation Dosage Code Evaluation

Phase 1: SHIELDOSE-2 Radiation-Assessment Code

Steven J. Gentz/NESC
Langley Research Center, Hampton, Virginia

Insoo Jun
Jet Propulsion Laboratory, Pasadena, California

National Aeronautics and
Space Administration

Langley Research Center
Hampton, Virginia 23681-2199

July 2023

Acknowledgments

The assessment team is grateful to the space-radiation technical community for their assistance and contributions, and particularly to peer reviewers Kerry Lee (Aerospace) and Neal Nickles (Ball Aerospace), and NESC reviewers Jon Holladay (GSFC), Elliott Cramer (LaRC), Heather Koehler (MSFC), and Tim Barth (NESC Integration Office).

Available from:

NASA STI Program / Mail Stop 148
NASA Langley Research Center
Hampton, VA 23681-2199
Fax: 757-864-6500

NASA Engineering and Safety Center
Technical Assessment Report

Space-Shielding Radiation Dosage Code Evaluation
Phase 1: SHIELDOSE-2 Radiation-Assessment Code

TI-21-01718

NESC Lead: Steven J. Gentz/NESC

Technical Lead: Insoo Jun/JPL

July 13, 2023

Report Approval and Revision History

NOTE: This document was approved at the July 13, 2023, NRB.

Approved: TIMMY WILSON Digitally signed by TIMMY WILSON Date: 2023.07.18 10:01:28 -04'00'

NESC Director

Version	Description of Revision	Office of Primary Responsibility	Effective Date
1.0	Initial Release	Steven Gentz, NESC Chief Engineer's Office, MSFC	07/13/2023

Table of Contents

List of Figures

List of Tables

Technical Assessment Report

1.0 Notification and Authorization

Emily Willis of the Marshall Space Flight Center (MSFC) Natural Environments Branch requested the NASA Engineering and Safety Center (NESC) provide an independent assessment of the National Institute of Standards and Technology (NIST) computer code SHIELDOSE-2 (1994) used to determine space-shielding radiation dose predictions to materials. This request was based on concerns on the accuracy and range of applicability of SHIELDOSE-2, which may not sufficiently be addressed in existing literature. Additionally, NASA programs and their prime contractors are requesting suggested alternate tools when SHIELDOSE-2 is identified as not applicable.

The independent assessment received authority to proceed on January 13, 2022, and its plan was approved on February 3, 2022.

Key stakeholders for this effort include:

- MSFC Natural Environments Branch
- Space Environments – Radiation Dose Analysis/Transport Communities
- NASA programs including Space Launch System (SLS), Multipurpose Crew Vehicles (MPCV), Gateway, Human Landing System (HLS), spacecraft projects, and technology-development initiatives

2.0 Signatures

Submitted by:

Steven Gentz Digitally signed by Steven Gentz Date: 2023.07.17 17:26:04 -05'00'

Mr. Steven J. Gentz

Significant Contributors:

Jun, Insoo Digitally signed by Jun, Insoo Date: 2023.07.17 12:55:59 -07'00'

Dr. Insoo Jun

Signatories declare the findings, observations, and NESC recommendations compiled in the report are factually based from data extracted from program/project documents, contractor reports, open literature, and/or generated from independently conducted tests, analyses, and inspections.

3.0 Team Members

Name	Discipline	Organization
Core Team		
Steve Gentz	NESC Lead	LaRC
Insoo Jun	Technical Lead	JPL
Stephen Seltzer	SHIELDOSE-2 code developer	National Institute for Standards and Technology (NIST)
Hugh Evans	Radiation Dose Analysis Expert	European Space Administration (ESA)
Carl Wendorff	Radiation Dose Analysis Expert	JSC/Northrup Grumman
Tony Slaba	Radiation Physics and Transport Expert	LaRC
Tom Carstens	Radiation Dose Analysis Expert	GSFC
Peter Bertone	Radiation Dose Analysis Expert	MSFC
Jarvis Caffrey	Radiation Dose Analysis Expert	MSFC
Alexander Henderson	Radiation Dose Analysis Expert	MSFC
Michael Goodman	Natural Environment Expert	Peraton
Brian Zhu	Radiation Transport Expert	JPL
Luz Maria Martinez-Sierra	Radiation Transport Expert	JPL
Tim Barth	Model and Simulation Evaluation	KSC
Radiation Code Expertise		
Tom Jordan	NOVICE code developer	Experimental & Mathematical Physics Consultants (EMPC)
Brian Franke	ITS (Integrated Tiger Series) and prior version	Sandia National Laboratories (SNL)
Robert Singleterry	MCNP (Monte Carlo N-Particle Transport)	LaRC
Makoto Asai	Geometry and Tracking 4 (Geant4) Radiation for Space (GRAS)	Jefferson National Accelerator Facility
Giovanni Santin	GRAS/MULASSIS (Multi-Layered Shielding Simulation Software)	ESA
Ruben Garcia	FLUKA (Fluktuierende Kaskade)	European Organization for Nuclear Research (CERN)
Lawrence Heilbronn	PHITS (Particle and Heavy Ion Transport Code)	University of Tennessee
Tony Slaba	HZETRN (High-Z and Energy Transport)	LaRC
Remi Benacquista	FASTRAD	TRAD
Athina Varotsou	FASTRAD	TRAD
Jeremie Plewa	FASTRAD	TRAD
Consultants		
Joe Minow	Space Environments NASA Tech Fellow	MSFC
Emily Willis	Natural Environments	MSFC
Anthony Destefano	Natural Environments	MSFC
Erin Hayward	Radiation Materials Testing	MSFC
Piers Jiggens	Radiation Dose Analysis Expert	ESA
Mark Millinger	Radiation Dose Analysis Expert	JSC/ESA
Business Management		
John LaNeave	Program Analyst	LaRC/MTSO

Assessment Support		
Diane Sarrazin	Project Coordinator	LaRC/Barrios
Linda Burgess	Planning and Control Analyst	LaRC/AMA
Dee Bullock	Technical Editor	LaRC/AMA

3.1 Acknowledgements

The assessment team is grateful to the space-radiation technical community for their assistance and contributions, and particularly to peer reviewers Kerry Lee (Aerospace) and Neal Nickles (Ball Aerospace), and NESC reviewers Jon Holladay (GSFC), Elliott Cramer (LaRC), Heather Koehler (MSFC), and Tim Barth (NESC Integration Office).

4.0 Executive Summary

This Phase 1 task is to evaluate a radiation-assessment tool SHIELDOSE-2, especially for dose-computation applications for very thin (<0.254 mm or 10 mils) materials per request by the Artemis Program. Radiation-transport codes or radiation-analysis tools are used in the spacecraft-design community to define and assess the local radiation levels (e.g., components, materials, total ionizing dose (TID) effect etc.). In this assessment, the codes are not being evaluated for human or biological radiation exposure levels or resulting effects. Among various radiation-transport/analysis tools available, SHIELDOSE-2 is commonly used in the early spacecraft-design phases (e.g., concept development and preliminary design) because it has been established that it provides reasonably reliable results with relatively rapid computation time. Many NASA centers and programs/projects and their respective prime contractors, including those involved with Space Launch System (SLS), Multi-Purpose Crew Vehicle (MPCV), Gateway, and Human Landing System (HLS) Programs are using this tool. However, there are questions about the SHIELDOSE-2 radiation-analysis tool's accuracy and range of applicability, which may not be sufficiently documented in the existing literature. Specifically, it has been noted that there is a lack of knowledge or publicly available documents within the radiation community of experts on the:

1. Range of shielding thickness applicability,
2. Range of detector thickness applicability, and
3. Accuracy of shielding and target material density scaling that are not included in the SHIELDOSE-2 material database.

In this regard and per request by the Artemis Program, the NASA Engineering and Safety Center (NESC) initiated a two-phased study: (1) to better understand and document the SHIELDOSE-2 code capabilities and limitations, and (2) to recommend alternative tools to use for cases where SHIELDOSE-2 is not applicable. This report provides a summary of the Phase 1 study.

Key findings of the study are:

(1) SHIELDOSE-2 produces results to a shielding thickness of ~1 micrometer (μm) aluminum or equivalent, but the accuracy for such thin target[1] thickness has not been reported in the open literature. Therefore, SHIELDOSE-2 is not appropriate for use for thin shielding until more work is done to assess the accuracy. Here, thin shielding should be dependent on the specific problem being evaluated (i.e., low energy limit of input spectrum – see Section 7.1.4). Phase 2 of this study will attempt to provide more rigorous comparisons between SHIELDOSE-2 and a selection of representative radiation transport codes available in the community,

(2) SHIELDOSE-2 does not consider the effect of detector thickness when computing doses (i.e., Spencer-Attix cavity theory, where SHIELDOSE-2 calculation assumptions lead to results that pertain only to suitably small volumes of detector material in the aluminum absorber, such that the detector thickness is assumed to not affect the electron fluence spectrum in the subject sub-layer). Therefore, we infer that it is only appropriate to use for detectors where its thickness is about the continuous slowing-down approximation

[1] In this report, we define "Target Thickness" as the total thickness of material over which the transport calculation is being performed. On the other hand, "Detector Thickness" is the smallest thickness within the target over which the dose is being computed.

(CSDA) range corresponding to the lowest energy of the input spectrum. Related to this second finding, we suggest that other transport codes (e.g., those studied in Phase 2) should be used when the detector thickness is larger than the CSDA range of the lowest energy of the spectrum input and

(3) SHIELDOSE-2 does not employee density scaling. However, users may apply density scaling to the SHEILDOSE-2 results per their needs. When used for polytetrafluoroethylene (PTFE) Teflon™ and titanium, the dose estimates for materials other than aluminum based on the density scaling are within $\pm$25 % of the aluminum results in the material thickness and under the radiation environment relevant to this scope. For other cases (i.e., different thicknesses, different environments, different energies, etc.), the applicability of the density scaling should be investigated case-by-case.

5.0 Assessment Plan

The Phase 1 assessment reviewed the capability and limitation of the SHIELDOSE-2 radiation-analysis tool, especially in the light of the lack of documented knowledge on its validity range of thin materials (for this report, we define "thin" to be less than or equal 0.0254 cm (or 10 mil) aluminum). The Phase 1 assessment included: (1) a comprehensive review of SHIELDOSE-2 documents and related references, (2) investigating the validity of zero detector thickness assumed in SHIELDOSE-2 when estimating doses in various detector materials, and (3) a series of first-order simulations to understand the effect of typical density scaling for materials other than aluminum.

Phase 2 of this assessment, which will be contained in a separate report, will benchmark more complex non-Monte Carlo and Monte Carlo radiation-analysis codes appropriate to detailed spacecraft design and operational phases in the current and planned space environments (e.g., Marian, Jovian, etc.).

6.0 Introduction

The radiation-shielding analysis is a design process during which the local radiation environment at components within spacecraft (e.g., for device, material, sensors/detector, etc.) is being computed and defined. During this analysis, the ambient radiation environment is 'transported' to a specific location within the spacecraft to estimate the radiation level expected at that particular position. A variety of shielding/radiation transport codes[2] are available for this purpose in the space-radiation environments and shielding community. The specific use of each code is dependent on what radiation effect is being investigated and what level of modeling fidelity is desired for simulations (i.e., there is no 'one-size-fits-all' radiation transport code that can be used for all space-radiation shielding analyses). Ray-tracing tools with a low-fidelity geometric model might be sufficient in some cases, or more complex radiation transport codes with detailed geometry and comprehensive physics interaction models might be required in others. Careful consideration, planning, and experience are user prerequisites for these shielding/radiation-transport codes.

6.1 Radiation Effects

Space radiation is a key design consideration for any space mission. For non-human and biological experiments or payloads, radiation can cause damage or disruption to electronics, materials, and sensors/detectors through TID, displacement-damage dose (DDD), single event effects (SEE), or radiation-induced background noise in sensors/detectors. Internal and surface charging induced by space radiation can be important for certain missions, especially for those passing through the aurora region (i.e., surface charging) or those subjected to high-energy electron environments including electron radiation belts around Earth or Jupiter (i.e., internal charging).

[2] The term "radiation-transport codes" is being used in general sense in this report. In this instance, the definition of transport code is inclusive for those 'transporting' particles (e.g., Monte Carlo codes) and those which do not transport particles (e.g., ray-tracing tools).

6.1.1 Cumulative Effects

Among these radiation effects, TID as a cumulative effect can place demands on the spacecraft mass budget (e.g., shielding) and the allowable mission duration (i.e., lifetime TID exposure). DDD can have a similar cumulative effect on mission design for the subset of electronics that are susceptible to this dosage type. Whether the cumulative effect is TID or DDD, radiation-transport codes can be used to compute 'doses' (i.e., energy deposition in the material per mass) at specific spacecraft locations [ref. 1]. Furthermore, for internal-charging evaluation, the same codes are used to compute charge deposition (i.e., rate) within materials over their characteristic time scale [ref. 2].

6.1.2 Transient or Rate Effects

SEE is a transient effect in which a single particle with relatively high linear energy transfer (LET) can cause an ionization trail along the particle path in the sensitive volume within an electrical, electronic, and electromechanical device, sufficient to cause temporary changes in a circuit state or catastrophic system failures. In addition, for sensitive devices, secondary particles (e.g., neutrons) resulting from interactions with primary particles with spacecraft materials (e.g., high-energy protons) can induce SEEs. For detectors/sensors (e.g., charge-coupled devices, complementary metal-oxide semiconductors, micro-channel plates, etc.), the flux environment can generate radiation-induced noises that can temporarily degrade their functions. Radiation-transport codes can be used for estimating these phenomena. For example, Reference 3 provides a comprehensive review of the radiation-transport codes available for SEE and for other radiation effects. For surface charging, radiation transport is not necessary because this effect is computed based on the surface-current balance on a given surface.

6.2 Radiation-Analysis Tools

As discussed, radiation-transport codes are used to compute TID, DDD, SEE, noise background, and internal charging. Depending on the methodologies implemented, these transport codes can be classified into non-Monte Carlo and Monte Carlo categories. Generally speaking, non-Monte Carlo tools analytically determine the spatial/temporal evolution of source-particle energy spectra in mediums, while Monte Carlo tools obtain the source-particle energy spectra in mediums by simulating particle trajectories and sampling the physical interaction probabilities based on the relevant distribution functions (i.e., interaction cross sections). Typically, non-Monte Carlo tools perform the same prediction computationally faster than Monte Carlo tools.

Monte Carlo codes can be divided into forward and reverse or adjoint/time-reversal codes. Radiation-transport codes are desired to be versatile in their geometry-modeling capability and in being able to transport various particle species found in the space environment (e.g., electrons, protons, heavy ions, and secondary particles). Secondary particles can include neutral particles (e.g., neutrons and gamma rays). Accurate and reliable radiation-transport tools are needed for good shielding design, and many of these radiation-transport tools are available from the nuclear/radiation physics and space-radiation communities. Those include but are not limited to FASTRAD [ref. 4], NOVICE [refs. 12, 13], Monte Carlo for N-Particles (MCNP) [ref. 8], Geant4 [ref. 7], PHITS [ref. 41], and Fluktuierende Kaskade (FLUKA) [ref. 11]. The selection of a particular tool is typically application specific or user dependent. For example, FASTRAD and NOVICE are generally used for system-level TID calculations for components and materials, while MCNP, Geant4, FLUKA, and PHITS are typically used for a detailed treatment of particle-interaction physics (e.g., detector-response simulation).

Phase 2 of this assessment, published as a separate report, will benchmark a selection of these non-Monte Carlo and Monte Carlo radiation-analysis codes that are appropriate for detailed spacecraft design and operational phases in current and planned space environments (e.g., Marian, Jovian, etc.).

6.2.1 Non-Monte Carlo

There are a few non-Monte Carlo codes being used in the community (e.g., ray-tracing codes or sectoring-analysis methods), which use dose-depth curves to estimate low-fidelity TID or DDD levels at given locations. Note that ray-tracing codes are not 'transporting' particles. To calculate the dose received at a particular point, a specified number of straight rays are emitted from the dose point, distributed equally in all directions. For each of these rays, the encountered aluminum-equivalent thickness is computed. The dose received from each ray direction is interpolated from the aluminum dose-depth curve and a summation is performed over all directions. Dose-depth curves for a specific material can be generated using other Monte Carlo transport codes described in Sections 6.2.2 and 6.2.3. SHIELDOSE-2 is a code that can generate the dose-depth curves for selected materials [ref. 9] for specific geometries. Aside from these lower-fidelity ray-tracing codes, there is also the deterministic code HZETRN [refs. 5, 6]. It has been shown that the most recent three-dimensional (3D) version of HZETRN can fully reproduce Monte Carlo simulation results for muons, pions, neutrons, and protons if the same nuclear interaction cross sections are used and is able to analyze complex, fully detailed geometries relevant for space radiation protection.

6.2.2 Forward Monte Carlo (FMC)

FMC codes follow particles from the source to the targets where local radiation environments or dosimetry data are desired and resemble the physical processes. FMC codes are most efficient when the source is confined to a relatively small region and the targets are distributed in multiple locations. FMC codes have been developed mainly for nuclear physics, accelerator beam, and nuclear reactor communities. The use of these codes for space-radiation applications might not be numerically efficient if the radiation-source region is not confined in space and the target of interest is small compared to the overall spacecraft dimension (i.e., a bulk of the source particles will not be able to reach the target locations (i.e., being 'lost')). Thus, the main use of the FMC codes typically has been for beam-condition simulation, dose estimate in materials and devices, space-radiation detector design and numerical simulation, and nuclear-planetary sciences. However, with more powerful computing infrastructure, FMC codes are being increasingly used for applications in which dose computations are needed for relatively small components within large spacecraft.

Among available FMC codes, Geant4 [ref. 7], MCNP [ref. 8], Integrated Trans-Iron Galactic Element Recorder (TIGER) Series (ITS) [ref. 10], FLUKA [ref. 11], PHITS [ref. 41], and the FMC capability in NOVICE [refs. 1, 3, 4, 12, 13] and FASTRAD [ref. 4] might be additional code choices in the space-radiation transport community. These codes are 3D and have extensive particle-interaction physics options. Geant4, MCNP, FLUKA, NOVICE, and FASTRAD FMC can transport various types of radiation species while ITS is limited to electron and photon transport.

6.2.3 Reverse Monte Carlo (RMC)

RMC are sometimes referenced as Adjoint or backward-method codes that track particles in a time-reversal sense (i.e., from the targets to the source). These codes are efficient for cases in which the radiation source is dispersed in a large spatial scale and the radiation-effect computation is targeted in a small volume. This resembles the space-radiation transport situation. NOVICE is one of the most widely used RMC codes and was specifically developed for this situation [refs. 12, 13, and the NOVICE section in [ref. 3]]. As of this report writing, NOVICE and FASTRAD are the primary TID/DDD computation tools in the space-radiation shielding community.

More recently, RMC capabilities have been developed in Geant4 [ref. 14] which is available through the GRAS application [ref. 15]) and in the FASTRAD package [ref. 4]. Geant4 has been compared to other FMC and RMC codes to validate its usage for space-radiation shielding-design applications [refs. 1, 16].

6.3 Examples of Radiation-Shielding Analysis

Examples of space-radiation transport analysis for shielding design using these identified codes are abundant and can be found in many publications. Select representative references listed for identified application areas include:

1. Shielding analysis for Jovian missions [refs. 1, 17, 18, 19]
2. Shielding effectiveness of different materials and multiple layers for different environmental conditions. These include: [refs. 20, 21] for galactic-cosmic radiation (GCR), [ref. 22] for electrons and protons at geostationary equatorial orbit, [ref. 23] for high-energy electrons, and [ref. 24] for GCR and solar protons
3. Effects of proton-induced secondary particles [ref. 25, 26]
4. Secondary neutrons from GCR [ref. 27, 28]
5. Radiation environments at both commercial and military aviation altitudes [ref. 29]

The code choice for any specific problem is, on many occasions, dependent on each user's experience and preference. For example, when a monoenergetic electron beam condition is estimated to emulate the space electron-spectrum environment, the ITS one-dimensional (1D) module (i.e., TIGER) might be utilized because it is a benchmarked tool that is modeling a simple, computationally fast situation, and has accurate electron/photon transport physics [ref. 30]. This does not mean other 3D FMC codes cannot be used for this purpose. Monte Carlo codes are being used to perform event-by-event energy-deposition scoring in micrometric volumes, which is relevant for SEE calculations [refs. 3, 31].

6.4 Genesis of the Study and Problem Description

As discussed, some radiation assessment codes are most useful when a first-order TID and DDD estimate for components within a complex spacecraft structure is needed (e.g., FASTRAD or NOVICE ray-tracing). In different situations, other codes should be used if detailed particle interactions need to be accounted for in simulations (e.g., Geant4, MCNP, or FLUKA). However, these latter codes can be computationally demanding.

In this regard, first-order dose estimates are needed typically early in the spacecraft-design phase when the spacecraft's geometrical and compositional complexities are not well defined. In these instances, SHIELDOSE-2, which is not a ray-tracing or a transport code, can be useful for these first-order radiation estimations. SHIELDOSE-2 generates the dose-depth profile as a function of

aluminum shielding thickness for simple prescribed geometries (i.e., semi-infinite slabs, finite slabs, solid-sphere, and spherical-shell geometries) for an input radiation environment spectrum. Many NASA centers and programs/projects and their respective prime contractors, including those involved with SLS, MPCV, Gateway, and HLS Programs, are using SHIELDOSE-2 in lieu of using more complicated Monte Carlo or ray-tracing simulation tools. There is an added factor in which the 'learning curve' for the Monte Carlo and ray-tracing tools is greater than for SHIELDOSE-2, which results in a smaller radiation-assessment-code expertise pool.

However, there are questions about the SHIELDOSE-2 code accuracy and range of applicability that are not answered in the existing literature.

Specifically, it has been noted that there is a lack of knowledge or publicly available documentation within the radiation community of experts on the:

1. Range of shielding thickness applicability,
2. Range of detector thickness applicability, and
3. Accuracy of the density scaling approach when the dose-depth profiles in aluminum from SHIELDOSE-2 aluminum are used for other shielding materials.

In this regard and per request by the Artemis Program, NESC initiated a two-phased study: (1) to better understand and document the SHIELDOSE-2 code capabilities and limitations, and (2) to recommend alternative tools to use for cases in which SHIELDOSE-2 is not applicable. This particular report provides a summary of the Phase 1 study.

7.0 Analysis

7.1 Review of the SHIELDOSE-2 Capabilities and Limitations

This section is a synopsis of the information contained in Reference 9. This reference can be consulted for more detailed information concerning SHIELDOSE-2. This NESC assessment concerns thin target (i.e., < 0.254 mm) applications in which low-energy particles are considered the driving requirement. Other interaction phenomena (e.g., proton-induced nuclear reactions, bremsstrahlung, photo-nuclear reactions, etc.) are not discussed in detail. It is assumed that, based on the CSDA range consideration, electrons with < ~300 kilo-electron-volt (keV) and protons with < ~6 megaelectronvolt (MeV) are relevant for this assessment because when there is a mixed field of radiation with both low- and high-energy particles, for thin shields, lower-energy particles will be dominant in the energy deposition while the contribution from high-energy particles is less important. Even when the dose contribution from higher-energy particles is needed, the energy deposition from high-energy particles can be easily computed using the stopping power data, which is considered to be accurate. Therefore, the focus of this assessment is centered on understanding and describing lower-energy electron- and proton-dose calculations in SHIELDOSE-2. Discussion on proton-induced nuclear reactions and bremsstrahlung treatment in SHIELDOSE-2 is summarized for completeness. In addition, as the GCR environment contribution is negligible for the total-mission cumulative dose to materials given the comparatively intense exposure received from lower energy trapped electrons and protons; the transport of high-Z and high-energy GCR particles is therefore not discussed.

SHIELDOSE-2 was developed in the 1990s to provide for rapid calculations of absorbed dose as a function of depth in the aluminum-shielding material of spacecraft, given the electron and proton fluence spectra encountered in orbit. It has been predominately used for first-order dose

predictions when the spacecraft's geometrical and compositional complexities are not sufficiently defined (e.g., concept development and preliminary design).

The fundamental premise of the SHIELDOSE-2 dose computation model is based on the extensive usage of the pre-compiled electron and proton look-up tables. A detailed description of these tables is found later in this section. These tables are precalculated, mono-energetic depth-dose data for omnidirectional broad beams of electrons and protons incident on uniform aluminum media of simple plane slabs. Aluminum was selected as it represents a typical spacecraft structure material. The SHIELDOSE-2 database is a collection of tables that contains the dose-depth profiles for the omnidirectional and monoenergetic particles incident on the semi-infinite aluminum slabs. See Section 7.1.4 for implications related to this point. These data are being used within SHIELDOSE-2 with suitable transformations [ref. 32] to cover other geometries (e.g., finite slabs, solid spheres, and spherical shells). These monoenergetic results are used to predict the absorbed dose for proton/electron fluence spectra. In summary, SHIELDOSE-2 can provide the dose-depth distributions in aluminum for semi-infinite, finite, solid sphere, and spherical-shell geometries (Figure 7.1-1) for the given electron and proton input spectra. These dose-depth profiles can be an input to other radiation ray-tracing analysis tools (e.g., NOVICE or FASTRAD [ref. 4]). The SHIELDOSE-2 geometries are shown in Figure 7.1-1.

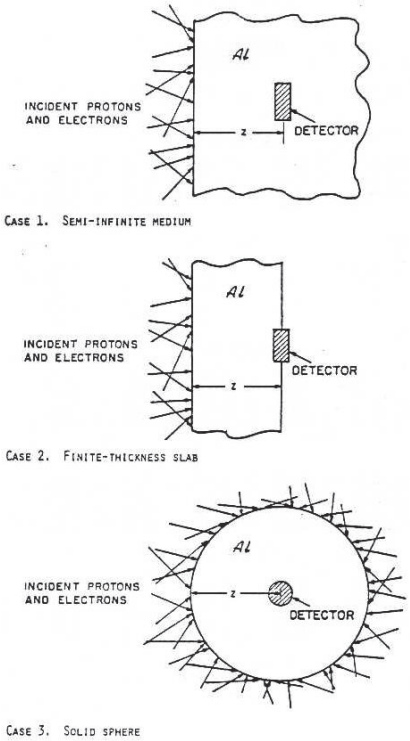

Figure 7.1-1. Geometries used in SHIELDOSE-2

As discussed, the essence to understand the operation, capability, and limitation of SHIELDOSE-2 would be to understand how the database has been created and is being used within this radiation assessment code [ref. 9].

7.1.1 Electron Component

Transport calculations to generate the SHIELDOSE-2 database for electrons and bremsstrahlung are based on the then-available cross-section information and Electron TRANsport (ETRAN) Monte Carlo code [ref. 33]. An additional reference for ETRAN is [ref. 34 – Chapters 7, 8, and 9], where the history of its development, select benchmarking results with experimental data, and agreements with the experimental data for different test cases were shown. As for ETRAN's verification and validation, it may be sufficient to note that in Reference 34 Chapter 8, there is a statement indicating *"From many comparisons in this paper, one gets the overall impression that the compromises embodied in the ETRAN Monte Carlo model are satisfactory and that the predictions made with the ETRAN code are reliable.*" In Phase 2 of this assessment, a more comprehensive comparison will be performed with other transport codes. The ETRAN code accounted for energy-loss straggling, multiple-elastic scattering angular deflections, the production, and transport of all generations of knock-on electrons, bremsstrahlung photons, and characteristic X-rays and Auger electrons subsequent to ionization events. The Monte Carlo results cover incident-electron kinetic energies from 0.005 to 50 MeV and extend to aluminum depths of 50 g/cm^2. This thickness deems sufficiently thick for all electron energies expected in space missions. Calculations were performed for an incident angular distribution that corresponds to an isotropic fluence of electrons incident on a semi-infinite plane slab aluminum target, with monoenergetic initial kinetic energies of 0.005, 0.01, 0.02, 0.05, 0.1, 0.2, 0.5, 1.0, 2.0, 5.0, 10.0, 20.0, and 50.0 MeV. Each run was based on the analysis of 100,000 incident electron histories, with radiations followed until they escaped the target, or their energy fell below 0.001 MeV. Scores were kept of the absorbed dose and the forward- and backward-directed electron fluence spectra as a function of depth to 1.25 times the CSDA electron range. In each table for a given incident electron energy, the aluminum slabs were divided into 50 sub-layers (i.e., the layer thickness is 0.025 of the CSDA electron range), and the computed doses are reported for each sub-layer. As the bremsstrahlung component was developed to be added to the electron component, secondary electrons from bremsstrahlung photons were not included in these scores.

The absorbed dose and the forward-directed and backward-directed fluence spectra of electrons were computed by using the ETRAN code as a function of depth out to 1.25 times the mean electron range. The absorbed-dose distributions in the semi-infinite aluminum plane slab targets were scaled and smoothed as functions of both depth z and incident energy using least-square cubic splines. To convert these depth-dose distributions to those for detector volumes other than aluminum and for finite-thickness aluminum slabs, the cavity theory of Spencer and Attix was used. Here, the cavity is assumed to be of small size so as not to perturb the electron fluence.

In addition to the absorbed dose in aluminum, SHIELDOSE-2 can evaluate the dose in small volumes of graphite, silicon, air, bone, calcium fluoride, gallium arsenide, lithium fluoride, silicon oxide, biological tissue (such as striated muscle), or water. For detector materials other than aluminum, the electron doses were computed using Eq. (1) and (2) in Reference 9, which are based on Spencer-Attix cavity theory and repeated in Figure 7.1-2. Electron stopping powers used in Figure 7.1-2 equations were calculated according to the methods given in ICRU Report 37 [ref. 35]. Note again that SHIELDOSE-2 calculation assumptions lead to results that pertain only to suitably small volumes of detector material in the aluminum absorber, such that the detector thickness is assumed to not affect the electron fluence spectrum in the subject sub-layer. Furthermore, as indicated earlier in the report, we are not evaluating SHIELDOSE-2 and other

Monte Carlo radiation codes for applications to human or biological radiation exposure levels or resulting effects.

Then for semi-infinite slabs,

$$\frac{D_{\infty}^{det}(z,T_o)}{D_{\infty}^{Al}(z,T_o)} = \frac{\int_{\Delta}^{T_o} F_e^{tot}(T,z,T_o)\left[\frac{L(T,\Delta)}{\rho}\right]^{det} dT + F_e^{tot}(\Delta,z,T_o)\left[\frac{S(\Delta)}{\rho}\right]^{det}\Delta}{\int_{\Delta}^{T_o} F_e^{tot}(T,z,T_o)\left[\frac{L(T,\Delta)}{\rho}\right]^{Al} dT + F_e^{tot}(\Delta,z,T_o)\left[\frac{S(\Delta)}{\rho}\right]^{Al}\Delta}, \quad (1)$$

and for finite-thickness slabs,

$$\frac{D_{-}^{det}(z,T_o)}{D_{\infty}^{Al}(z,T_o)} = \frac{\int_{\Delta}^{T_o} F_e^{for}(T,z,T_o)\left[\frac{L(T,\Delta)}{\rho}\right]^{det} dT + F_e^{for}(\Delta,z,T_o)\left[\frac{S(\Delta)}{\rho}\right]^{det}\Delta}{\int_{\Delta}^{T_o} F_e^{tot}(T,z,T_o)\left[\frac{L(T,\Delta)}{\rho}\right]^{Al} dT + F_e^{tot}(\Delta,z,T_o)\left[\frac{S(\Delta)}{\rho}\right]^{Al}\Delta}, \quad (2)$$

Figure 7.1-2. Equations Used for Computing Electron Doses in Sub-Layers Note, $F_e(T,z,T_o)$ is the electron fluence spectrum (forward and total, as indicated) as a function of kinetic energy T and depth z, $L(T,\Delta)/\rho$ is the electron restricted mass collision stopping power, restricted to energy losses less than Δ, $S(T)/\rho$ is the unrestricted mass collision stopping power, and Δ is a cut-off energy generally associated with the cavity size. The values of Δ were chosen as max(T_o/5000, 1 keV), which places them between 10 and 1 keV.

The SHIELDOSE-2 thickness applicability would be related to the energy ranges covered for the ETRAN-created database (i.e., dose tables). As stated, the maximum SHIELDOSE-2 thickness is 50 g/cm^2. However, the lowest applicable SHIELDOSE-2 thickness is not explicitly stated and must be inferred. The lowest SHIELDOSE-2 electron energy considered is 0.005 MeV. Table 7.1-1 presents the CSDA ranges for select electron energies from the SHIELDOSE-2 database. Since the range for the 0.005-MeV electrons is used for the electron table total thickness for the 0.005 MeV electron (i.e., 1.25 times the 0.005-MeV electron range), and the table is divided into 50 sub-layers, the SHIELDOSE-2 can provide a dose number to 1/50 of the 5-keV electron range. The main message is that SHIELDOSE -2 would provide answers even for sub-μm thicknesses in the order of 1/50 of ~0.4 μm for the electron incident cases (i.e., 0.008 μm) although the accuracies for such thin applications have never been studied or reported. Even after an extensive search and consulting with many experts in this field (including the team members of this assessment), we were only able to find one conference paper [ref. 36] where it was shown that the SHIELDOSE-2 results diverge from the TIGER results for < 0.01 cm (or 4 mil) of aluminum for a particular environment they used, which stops at ~50 keV at the lower end of the spectrum. To better quantify the accuracy of SHIELDOSE -2 results for thinner material application, more work is needed, which is the main objective of Phase-2 of this assessment.

Table 7.1-1. Electron CSDA Ranges Used in SHIELDOSE-2 for Select Energies in Various Units

	0.005 MeV e-	**0.01 MeV e-**	**0.1 MeV e-**	**1 MeV e-**	**7 MeV e-**
g/cm^2	1.092E-04	3.539E-04	1.872E-02	5.546E-01	4.242E+00
cm	4.044E-05	1.311E-04	6.933E-03	2.054E-01	1.571E+00
mil	1.592E-02	5.161E-02	2.730	8.087E+01	6.285E+02
μm	4.044E-01	1.311E+00	6.933E+01	2.054E+03	1.571E+04

7.1.2 Bremsstrahlung Component

The ETRAN Monte Carlo calculations were performed in a fashion similar to that for the electron component, treating the same set of monoenergetic incident electron kinetic energies, followed down to an energy of 1 keV. The calculation treats the photon interactions of pair and triplet production, incoherent/Compton scattering, coherent scattering, and photoelectric absorption. Secondary charged particles were followed to include their contribution to the bremsstrahlung component. The photon fluence spectra were scored to depths of 50 g/cm^2 of aluminum. With the assumption of charged-particle equilibrium, the bremsstrahlung doses were computed by integrating the photon spectra times the mass attenuation coefficients (μ_{en}) for the selected detector material. Eqs. (3)-(5) in Reference 9 illustrate how the computations are conducted in SHIELDOSE-2. The mass attenuation coefficients used in these equations were obtained from calculations outlined in Reference 37. The μ_{en} ratio scaling and smoothing were performed to facilitate interpolation. The photon spectra averaged over each aluminum sub-layer were calculated for use in those equations.

7.1.3 Proton Component

Depth-dose distributions were calculated for an isotropic fluence of protons incident on a semi-infinite plane slab aluminum target, with monoenergetic initial kinetic energies of 0.01, 0.015, 0.02, 0.03, 0.04, 0.05, 0.06, 0.08, 0.1, ... , 1000, 1500, 2000, 3000, 4000, 5000, 6000, 8000, and 10000 MeV. The information on proton stopping powers and ranges in the materials of interest has been taken from the then-recent ICRU Report [ref. 38]. For proton transport, the straight-ahead (i.e., neglect of elastic-scattering angular deflections) and continuous-slowing-down (i.e., neglect of energy-loss straggling) approximations were used in SHIELDOSE-2, from which the depth dose can be calculated from a relatively simple numerical evaluation. Scores of the absorbed dose and the forward-directed fluence spectra of protons as a function of depth to 1.0 times the mean proton range were calculated. In each table for a given incident proton energy, the aluminum slabs are divided into 50 sub-layers resulting in a thickness of 0.02 of the CSDA proton range, with the computed doses reported for each sub-layer. The proton doses were computed using Eq. (6) in Reference 9 in which the proton spectra averaged in each aluminum sub-layer and the proton mass stopping powers were used.

As with the electron case, the SHIELDOSE-2 thickness applicability is closely related to the proton energy range covered when the database (i.e., depth-dose tables) was created. Table 7.1-2 shows the CSDA ranges for select proton energies from the SHIELDOSE-2 database. The SHIELDOSE-2 lowest proton energy range (i.e., 0.01 MeV) is less than 1 μm, which is divided into 50 sub-layers in the 0.01 MeV proton database. Therefore, the proton thickness applicability is 1/50 of ~0.2 μm, or 4E-3 μm.

Overall, when the electron and proton ranges are combined, it can be assumed SHIELDOSE-2 can be used to estimate the doses for sub-μm aluminum thicknesses although the accuracy of the results cannot be accessed at this time.

Table 7.1-2. Proton CSDA Ranges Used in SHIELDOSE-2 for Select Energies in Various Units

	0.01 MeV p	**0.1 MeV p**	**1 MeV p**	**7 MeV p**	**100 MeV p**
g/cm^2	5.94E-05	2.63E-04	3.95E-03	9.21E-02	9.98E+00
cm	2.20E-05	9.75E-05	1.46E-03	3.41E-02	3.69E+00
mil	8.66E-03	3.84E-02	5.75E-01	1.34E+01	1.45E+03
μm	2.20E-01	9.75E-01	1.46E+01	3.41E+02	3.69E+04

Dose estimates from the proton-induced nonelastic nuclear reaction products are an approximation in SHIELDOSE-2 in that rigorous particle interactions were not followed in the computation. Rather, SHIELDOSE-2 used the knowledge of the total nonelastic-nuclear-interaction cross-section to compute the proton energy attenuation in aluminum and assumed that the charged-particle nuclear secondaries are absorbed at the point of production. The energy converted to secondary neutron energy and de-excitation gamma-ray energy cannot be assumed locally absorbed. Therefore, SHIELDOSE-2 considered two options: (1) to assume that such energy escapes the region of interest, and (2) to assume the total neutron energy produced by the incident proton is exponentially distributed from the entrance surface with an aluminum attenuation coefficient of 0.03 cm^2/g. As noted in Reference 9, because there are uncertainties associated with the treatment of nuclear-interaction effects and the dose ratios used to convert to dose in detector materials other than aluminum, it is recommended that reliance not be placed on the use of these approximations but used perhaps to gauge possible effects that might require more accurate follow-up. For example, Bragg peaks are not reproduced. It should be recalled that only the physically absorbed dose has been addressed. High-LET effects associated with heavier secondaries are beyond the scope of this assessment. It also should be further noted that nuclear reactions should not be an appreciable contributor to doses for thin shielding cases such as our assessment scope (<~0.0254 cm or 10 mil). For example, protons should have kinetic energies > 20 MeV to be able to initiate nuclear reactions in silicon. Therefore, its importance related to this assessment will be ignored.

7.1.4 General Notes

SHIELDOSE-2 users are required to provide electron and proton input spectra for their specific environmental applications. As for the thickness applicability, while it has been discussed that the SHIELDOSE-2 database is applicable to below sub-μm thicknesses, the thickness applicability is also closely related to the lower energy limits of the input spectra defined by the users. If the users do not provide the spectrum information down to sufficiently low energy to cover their intended thickness application, then SHIELDOSE-2 would extrapolate the input spectra to the lower energies using a log-cubic-spline fit and the results would be unreliable. It may be a good general practice to specify the lowest energy limit that matches the material thickness over which the doses are being computed. However, specifying the lowest energy limit for a given design case might involve an engineering judgment between the material thickness and the environment model(s) available. For example, if one wants to compute the dose in a 0.00254-cm (or 0.006858-g/cm^2 or 1-mil-thick aluminum), the lowest energy point of the input spectrum should be at least ~0.05 MeV for electrons (CSDA range = 0.005738 g/cm^2) and ~1.25 MeV for protons (CSDA range = 0.005509 g/cm^2). Or for 1-μm-thick (or 2.70E-4 g/cm^2) aluminum, they should be ~0.008 MeV electrons (CSDA range = 2.418E-4 g/cm^2) and ~0.1 MeV protons (CSDA range = 2.63E-4 g/cm^2). In some cases, the uncertainty of radiation environment specifications dominates the SHIELDOSE-2 result uncertainties because it is a general consensus of the community that the uncertainties associated with the environment models are ‘typically’ larger than the uncertainties associated with the radiation-transport calculations, especially for low-energy environment models. For example, in many cases when sufficient radiation design margin (RDM) is demonstrated even from a simple transport calculation (e.g., when the SHIELDOSE-2 analysis shows we already meet the RDM requirement), then we do not typically perform additional (more sophisticated) transport simulation to improve the margin. This is because the design margin requirement is sufficient to

cover the environment uncertainty. Therefore, as long as even a simple shielding analysis shows that the RDM requirement is met, there is no need to improve the transport code calculation.

SHIELDOSE-2 as originally distributed has a poorly documented error in its database which many implementations (e.g., SPENVIS and SHIELDOSE-2Q) have corrected. The database swaps the non-aluminum bremsstrahlung tables for the semi-infinite and finite slab cases. The error caused by this is insignificant for the most common use cases but could be significant in some scenarios. If bremsstrahlung is expected to be a significant contribution to the total dose, the user should either correct the error if using SHIELDOSE-2 directly or confirm that their implementation has done so.

The spherical case doses output by SHIELDOSE-2 are based on hemispherical radiation and thus must be multiplied by 2 for isotropic radiation across the whole sphere. While this is properly stated in the output when using SHIELDOSE-2 directly, the published documentation for SHIELDOSE-2 incorrectly implies the full sphere is considered. Thus, when using SHIELDOSE-2 as part of a larger system care should be taken to confirm whether the factor of 2 has been incorporated.

7.2 Density-Scaling Investigation

Because the radiation transport and shielding analysis are strongly dependent on the problem geometry (slab in our case) and the radiation environment under which the material is subjected to (low energy environment in our case), we focus the assessment for thin slab material (i.e., 25.4 μm or 0.006858 g/cm^2 aluminum). That is, the simulation results and interpretation of them in this and the next section will be mainly for thin <~0.0254 cm (or 10-mil) materials subjected to program-specific Design Specification for Natural Environments (DSNE), which is most relevant for thin material applications (e.g., Gateway Program). In this scenario, the low-energy particles will be mostly responsible for the energy deposition in thin regions. For example, 1-mil (or 25.4-μm) aluminum corresponds to the CSDA range of ~55 keV electrons or ~1.3 MeV protons, and 10-mil (or 254-μm) aluminum corresponds to the CSDA range of ~220 keV electrons or ~6 MeV protons. This implies that higher-energy particles (e.g., GCR and solar energetic particles) will nominally pass through the material while depositing some energies per the corresponding LET values.

As discussed, aluminum is the only shielding material considered in SHIELDOSE-2. Then, for other detector materials, SHIELDOSE-2 computes the doses using the spectra computed for the aluminum medium (see Equations in Figure 7.1-2), but with the stopping power for that specific detector material of interest. In the radiation-effect community, when encountered with different shielding media other than aluminum, density scaling is commonly used as an approximation, where actual material thicknesses are converted to the equivalent aluminum thickness using the density ratio. For example, 1 cm of PTFE Teflon™ with a bulk density of 2.2 g/cm^3 can be approximated by ~0.81 cm of aluminum with a density of 2.7 g/cm^3 or 0.489 cm of titanium with a density of 4.5 g/cm^3. In this way, the dose-depth distributions computed by SHIELDOSE-2 can be converted to the dose-depth distributions in other shielding materials. Note ‘fluence spectra’ used in the dose computations are still for the aluminum medium.

Independent of SHIELDOSE-2, a series of first-order Geant4 Monte Carlo simulations were performed to understand how the dose-depth profiles change as a function of the same areal density (i.e., g/cm^2) for aluminum, titanium, and PTFE Teflon™. Note that the Geant4 results shown provide a check on the applicability of the density scaling. While SHIELDOSE-2 dose-

depth profiles can be compared with the Geant4 dose-depth profiles, it will not be really a check on the density scaling as it will be just a comparison between SHIELDOSE-2 and Geant4. The computations are done with the omnidirectional, isotropic (cosine-law source) of electron (and proton spectra) in a simple slab geometry. As discussed, the assessment used the environment defined in the Gateway Program DSNE for the fluence of electrons and protons from the solar wind and Earth's magnetotail. The electron and proton spectrum inputs are adopted from Figure 3.3.1.10.2-5 and Table 3.3.1.10.2-6 in the DSNE Revision I [ref. 39]. In Geant4, the absorbed doses are computed from the balance between incoming energy and outgoing energy in each layer. The Geant4 physics lists used in the simulations were the electromagnetic (EM) Option 4 for EM physics and FTFP_BERT_HP for hadronic physics[3]. Thus, the results described are the doses in the specific material. For example, the dose profile for PTFE is the doses computed in PTFE with particles being transported in PTFE. The results are shown in Figure 7.2-1 for electrons and in Figure 7.2-2 for protons. The figures in the left column are the actual dose-depth profiles and the figures in the right column are the dose ratios to the aluminum doses at the same areal density.

Figure 7.2-1 shows the results for the electron spectrum input case to 0.6858-g/cm^2 or 0.254-cm depth. Note the Gateway Program DSNE electron spectrum spans the energy from 1 eV to ~7 MeV. The CSDA range of 7-MeV electrons in aluminum is 4.242 g/cm^2 or 1.571 cm. However, the simulation was performed for a slab thickness of 0.254 cm (or 100 mils). The slab is divided into 1000 layers, which means that the thickness of each layer is 2.54-μm Al or 6.858E-4-g/cm^2. The result indicates the density scaling between different materials are within ~25% of each other.

Figure 7.2-2 shows the results for the proton-spectrum input case for a slab of 0.254 mm or 0.06858 g/cm^2 aluminum. The Gateway Program DSNE specifies the proton spectrum from 1 eV to ~7 MeV, and the CSDA range of 7-MeV protons is 0.0921 g/cm^2 or 0.0431 cm in aluminum. The proton-spectrum simulation was conducted for a 0.254-mm (or 10-mil) aluminum slab divided into 1000 layers. Two distinct features are apparent, which were not found in the electron-spectrum case. First, the doses at the 'shallow' region (i.e., within the first few layers) are large and decrease rapidly as a function of thickness. This is because low-energy protons (i.e., < 0.1 MeV) stop at these shallow regions. For example, as noted in Table 7.1-2, the CSDA range of 0.01 MeV protons is 5.94E-5 g/cm^2 or 0.220 μm in aluminum, and the thickness of each layer is 6.858E-5 g/cm^2. Hence, protons with energy < 0.01 MeV would stop in the first layer of aluminum resulting in an elevated dose. The dose ratios to aluminum at the first few layers are large even at the same areal density. Note that the areal thickness of 6.858E-5 g/cm^2 corresponds to 0.254 μm aluminum, 0.312 μm PTFE Teflon™, or 0.152 μm titanium thickness. At this shallow region, the simulation results indicate the thickness seems more important and the density scaling breaks down. Second, as the areal thickness increases, the dose ratios start to rapidly diverge. This is because of the Bragg-peak effect.

Figure 7.2-3 shows the dose profile and the ratios for the combined electron and proton spectra. The simulations were performed for a 0.254-cm (or 100-mil) aluminum slab or equivalent, divided into 1000 layers. Interestingly, because the electron dose dominates the total dose for the bulk of the material thickness, the dose-ratio plot for this combined-spectrum case follows the pattern of the electron-spectrum case shown in Figure 7.2-1 and agrees within ±25%. For this

[3] https://geant4-userdoc.web.cern.ch/UsersGuides/PhysicsListGuide/html/index.html

particular application in which the DSNE radiation environment was used, the density scaling appears valid within ±25% from ~ 25.4 to 2540 μm aluminum or equivalent. However, this might not hold true for other environments where low-energy protons dominate the dose.

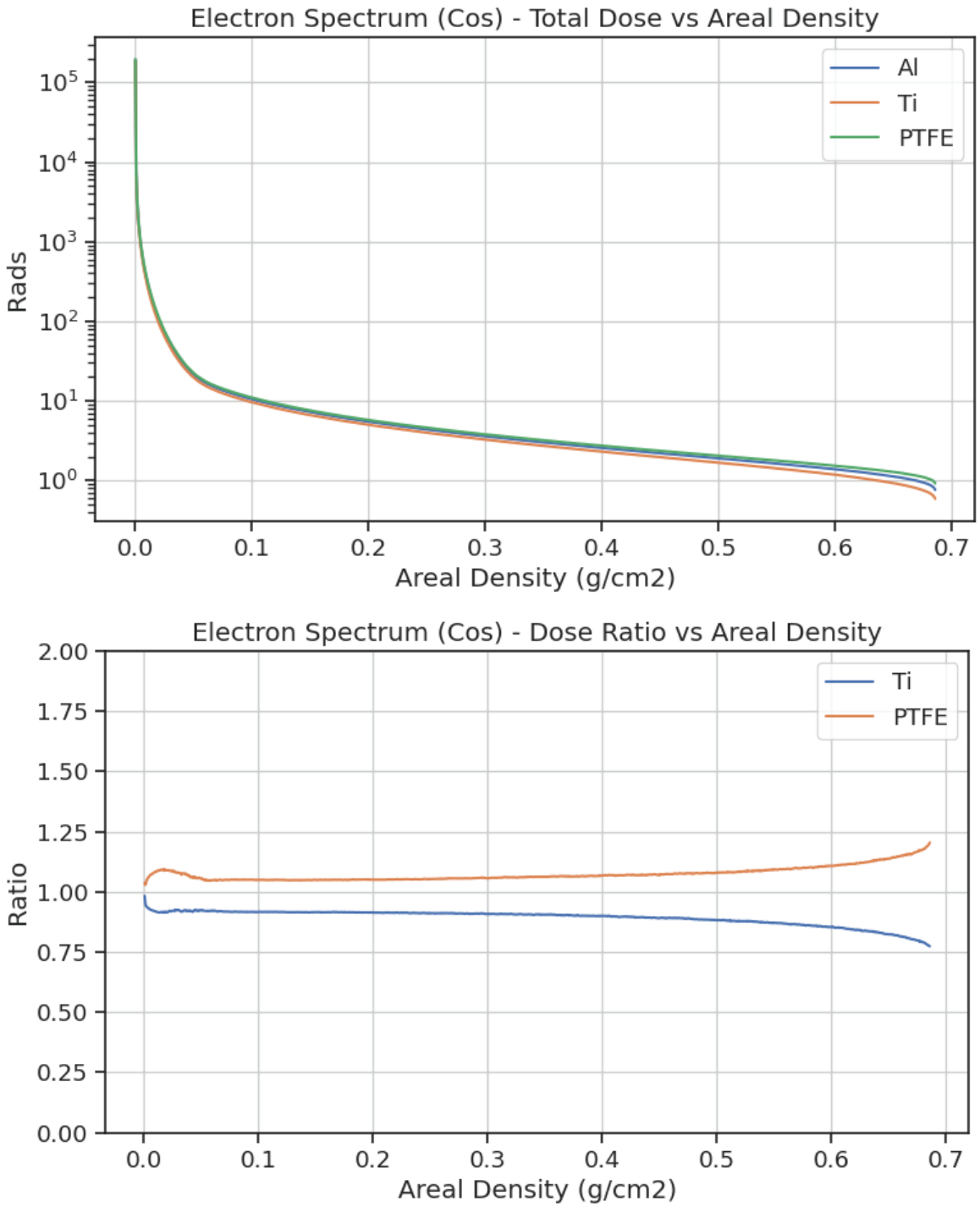

Figure 7.2.-1. Geant4 Simulation Results for the Electron Dose-Depth Distribution as a Function of Areal Density (g/cm^2) for Aluminum, Titanium, and PTFE Teflon™ for Spectrum Input The cosine-law angular distribution has been used for the electron sources impinging into a slab. The plot in the top is for the dose-depth profiles and the plot in the bottom is for the ratios to the aluminum doses at the same areal density.

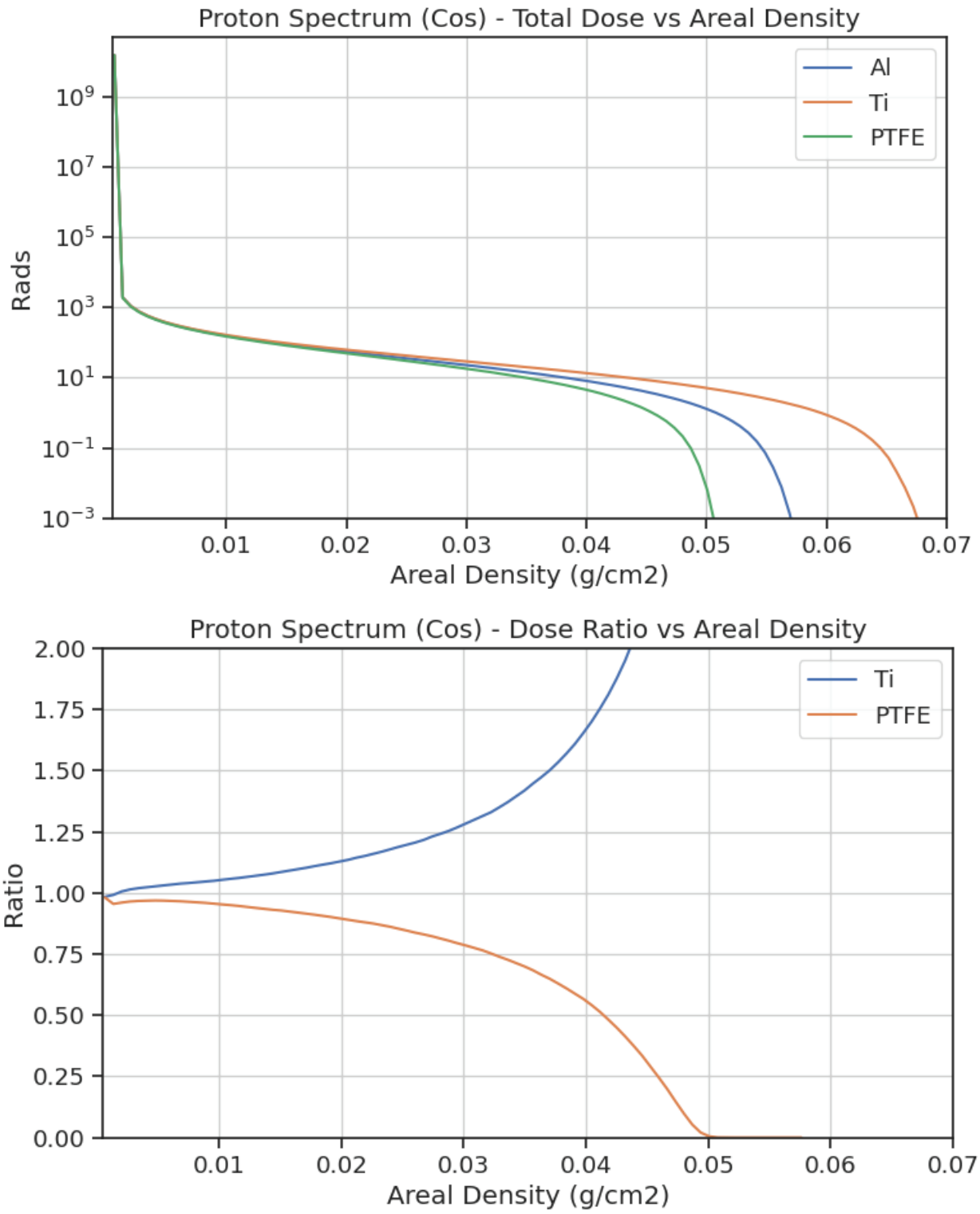

Figure 7.2-2. Geant4 Simulation Results for the Proton Dose-Depth Distribution as a Function of Areal Density (g/cm^2) for Aluminum, Titanium, and PTFE Teflon™ for Spectrum Input
The cosine-law angular distribution has been used for the proton sources impinging into a slab. The plot in the top is for the dose-depth profiles and the plot in the bottom is for the ratios to the aluminum doses at the same areal density.

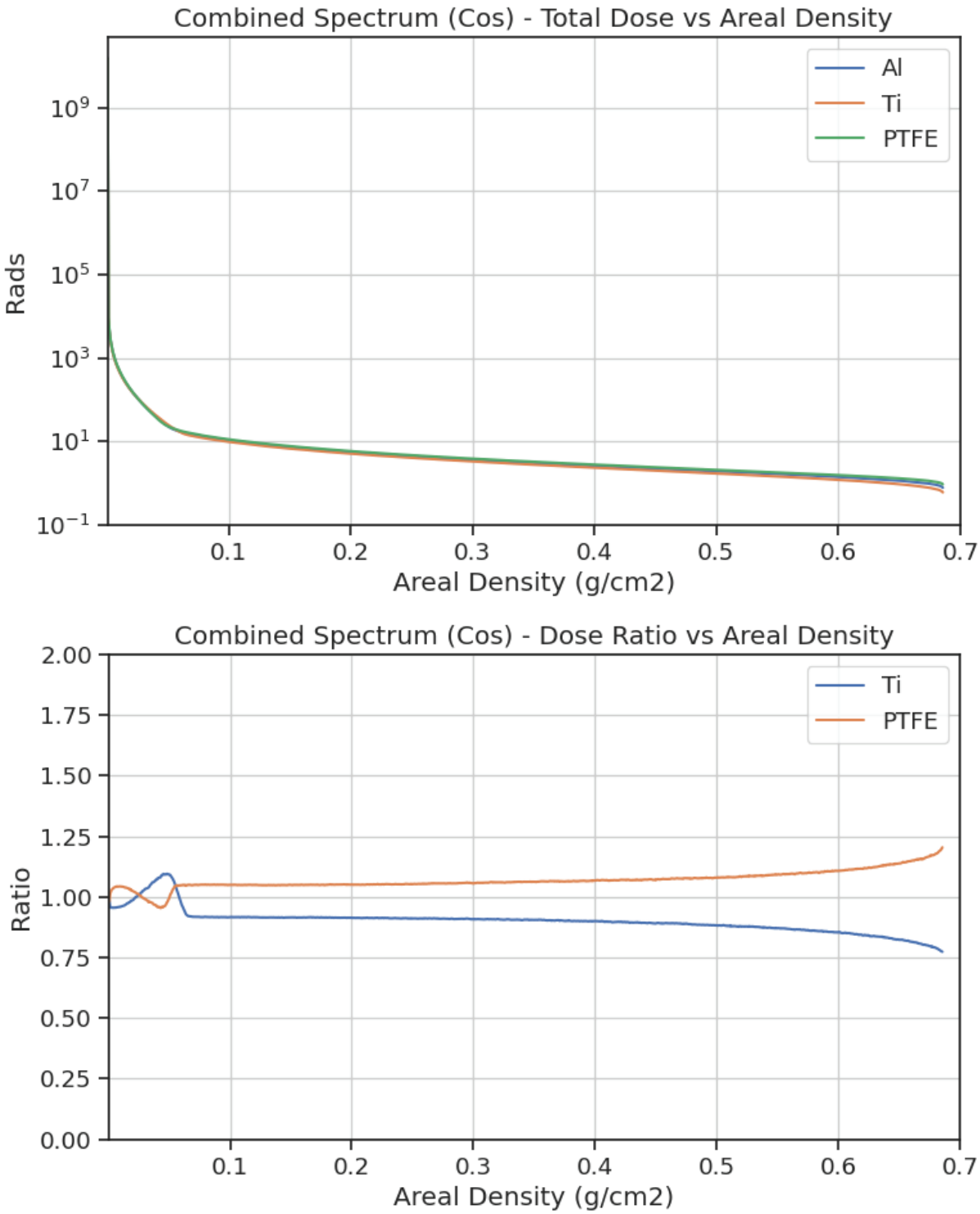

Figure 7.2-3. Geant4 Simulation Results for the Combined Electron and Proton Spectrum Dose-Depth Distribution as a Function of Areal Density (g/cm^2) for Aluminum, Titanium, and PTFE Teflon™
The cosine-law angular distribution has been used for the particle sources impinging into a slab. The plot in the top is for the dose-depth profiles and the plot in the bottom is for the ratios to the aluminum doses at the same areal density.

It should be noted the density scaling is not an inherent SHIELDOSE-2 capability, and it does not guarantee the correct result after the thickness conversion. As described, SHIELDOSE-2 uses the pre-computed lookup tables of dose-depth profiles that are stored for many mono-energetic cases. The dose values in the tables were computed by ETRAN for the aluminum medium and its LET. For detector materials other than aluminum, SHIELDOSE-2 uses the particle spectrum computed for aluminum medium but uses the LET values of a detector material of interest. If the density scaling is applied to the SHIELDOSE-2 results, then the particle spectra computed for aluminum would be used for different thicknesses of different materials. Users of the density scaling of the SHIELDOSE-2 results should be aware of this result for their specific applications. When an accurate dose assessment is needed, a dose profile should be obtained for the material of interest using a more physics-oriented tool (e.g., Geant4, MCNP, PHITS, FLUKA, etc.).

7.3 Effect of Detector Thickness over which Doses are Calculated

In this section, two aspects of the target thickness effect on dose computation are discussed: (1) establishing the minimum detector thickness in SHIELDOSE-2, and (2) how the detector thickness variation would impact the dose computation results.

As introduced in Section 7.1, SHIELDOSE-2 calculations assume the detector thickness is thin such that the particle fluence spectrum in the subject sub-layer would not be modified in the sub-layer where the dose is being computed. This indicates the detector thickness should not affect the overall spectrum of the incoming particles after passing through the sub-layer. This implies the detector thickness should be about one CSDA range corresponding to the lowest energy point provided in the input spectrum. Although this is not a rigorous derivation of the required detector thickness for SHIELDOSE-2, it can be used as a general guideline when setting the SHIELDOSE-2 geometry input. This may be another area where user engineering judgment is needed.

Related to point (2), Geant4 simulation results are presented to investigate how the target thickness would impact the dose computation. It is somewhat obvious that the dose averaged over a finite target volume would be dependent on the target thickness because a portion of the incident particles would be absorbed in the material, and at the same time the particle incident energy will be modified and the associated stopping power (i.e., LET) will be correspondingly changing. The primary assessment intent is to ascertain how sensitive the dose computation would be dependent on the target thickness for different particle/energy incident cases. The main geometry is the same as that used in the density-scaling simulations with a total slab thickness of 0.254 cm which is divided into 1000 layers. The cosine-law angular distribution is used for all computations. The results are shown in Figure 7.3-1 for electrons and Figure 7.3-2 for protons. While not visible, each line in these figures consists of 1000 points, corresponding to 1000 doses computed. The first point of the figures is the dose in the first layer, the second point of the figures is the dose averaged over the first two layers, and the third point of the figures is the dose averaged over the first three layers, with the subsequent points averaged in the same method.

As expected, the thickness over which the doses are calculated has a strong effect on the results, especially for the shallow regions in the spectrum-input cases. This illustrates the material thickness consideration should be included in the dose computation and effect assessment. Supporting this finding, it has been noted [ref. 40] that detailed dose-depth profile could be simulated even for a thin material (i.e.,1 mil or 25.4 μm) and reproduced in ground laboratory conditions using multiple energy beams if the proper material degradation assessment is needed.

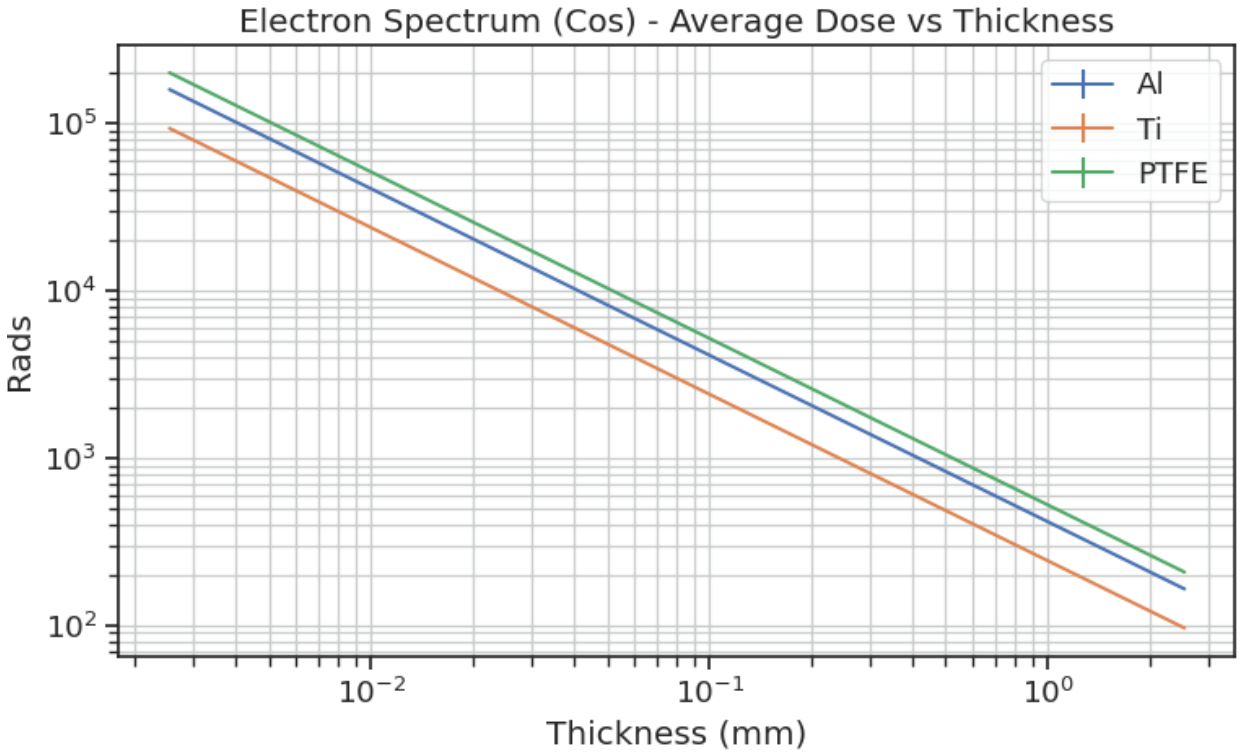

Figure 7.3-1. Geant4 Computed Doses as a Function of Target Thickness for Electron Spectrum Input

Each line in the figures consists of 1000 points, corresponding to 1000 doses computed. The first point of the figures is for the dose in the first layer, the second point is for the 'average' dose in the first two layers, with the subsequent points averages in the same progression. The cosine-law angular distribution has been used for the electron sources impinging into a slab.

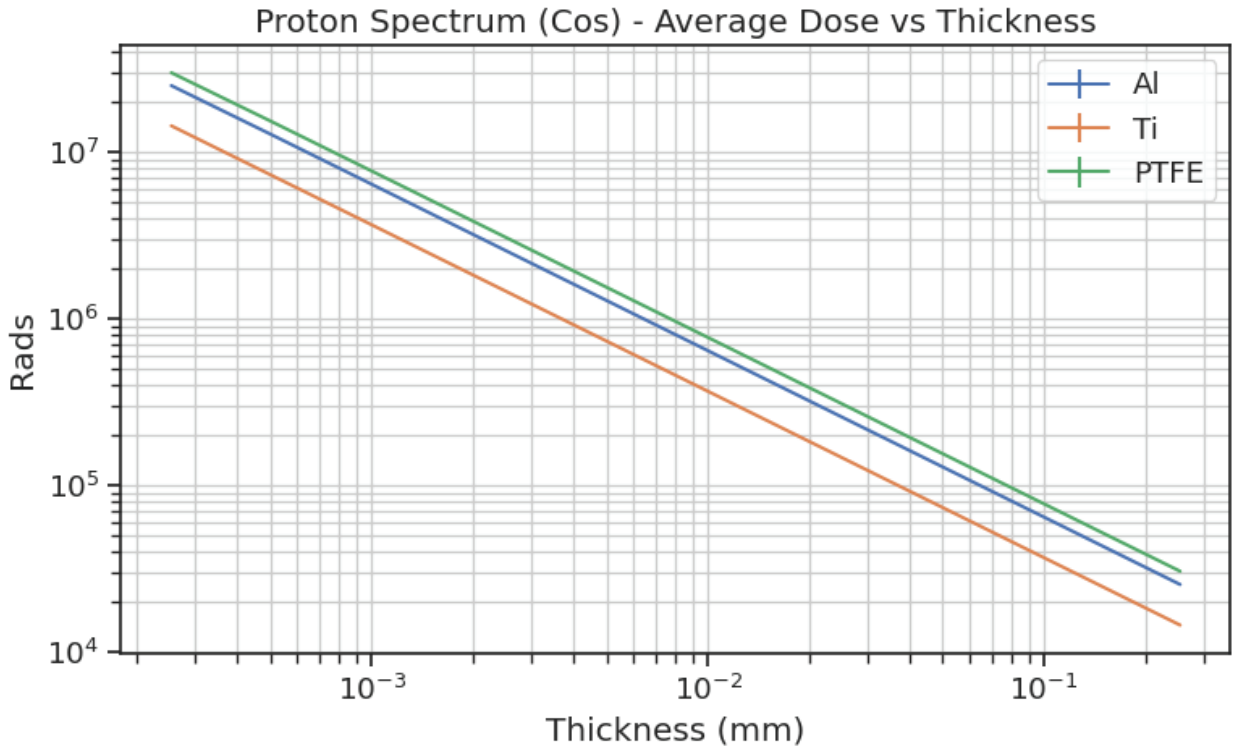

Figure 7.3-2. Geant4 Computed Doses as a Function of Target Thickness for Proton Spectrum Input
The first point of the figures is for the dose in the first layer, the second point of the figures is for the 'average' dose in the first two layers, with the subsequent points averages in the same progression. The cosine-law angular distribution has been used for the electron sources impinging into a slab.

8.0 Findings and Observations

8.1 Findings

F-1. SHIELDOSE-2 can provide results to the shielding thickness of ~1-μm depth although its accuracy and validity has not been addressed in the open literature. (Section 7.1)

F-2. SHIELDOSE-2 does not consider the effect of detector thickness when computing doses (i.e., Spencer-Attix cavity theory, where SHIELDOSE-2 calculation assumptions lead to results that pertain only to suitably small volumes of detector material in the aluminum absorber, such that the detector thickness is assumed to not affect the electron fluence spectrum in the subject sub-layer. (Section 7.1)

F-3. SHIELDOSE-2 does not use density scaling.

- Users may apply density scaling to the SHEILDOSE-2 results per their needs. When used for polytetrafluoroethylene (PTFE) Teflon™ and titanium, density scaling for different shielding materials provides results to within ±25% of the aluminum results up to 10 mils (or 0.254 mm) for the Gateway environment considered in this study. (Section 7.2).

- Note the applicability of density scaling for other types of environments and for thicker target material has not been addressed in this assessment.

F-4. Detailed dose-depth profile transport calculation is necessary if accurate dose computation is required for targets as thin as ~25.4 μm (or 1 mil). (Section 7.3)

8.2 Observations

O-1. Then-available ETRAN was used for SHIELDOSE-2 electron and bremsstrahlung radiation transport. (Section 7.1)

O-2. No transport calculations were performed for proton-incident case in SHIELDOSE-2. (Section 7.1)

O-3. SHIELDOSE-2 covers incident electron energies from 0.005 MeV to 50 MeV, with the bremsstrahlung tail calculated to depths of 50 g/cm^2, and incident proton energies from 0.01 MeV to 10 GeV. (Section 7.1)

O-4. The absorbed dose and the forward-directed and backward-directed fluence spectra of electrons were computed by using the ETRAN code as a function of aluminum depth to 1.25 times the mean electron range. To convert these depth-dose distributions to those for detector volumes other than aluminum and for finite-thickness aluminum slabs, the cavity theory of Spencer and Attix was used. (Section 7.1)

O-5. SHIELDOSE-2 uses a log-cubic-spline fit (extrapolation and interpolation) to define the unspecified energy range of the input spectrum. (Section 7.1)

O-6. In most cases, radiation-environment uncertainty (e.g., solar wind, trapped particles) is greater than transport uncertainty. (Section 7.1)

9.0 Alternate Technical Opinion(s)

No alternate technical opinions were identified during the course of this assessment by the NESC assessment team or the NESC Review Board (NRB).

10.0 Definition of Terms

Finding	A relevant factual conclusion and/or issue that is within the assessment scope and that the team has rigorously based on data from their independent analyses, tests, inspections, and/or reviews of technical documentation.
Observation	A noteworthy fact, issue, and/or risk, which is not directly within the assessment scope, but could generate a separate issue or concern if not addressed. Alternatively, an observation can be a positive acknowledgment of a Center/Program/Project/Organization's operational structure, tools, and/or support.
Recommendation	A proposed measurable stakeholder action directly supported by specific Finding(s) and/or Observation(s) that will correct or mitigate an identified issue or risk.

11.0 Acronyms and Nomenclature List

1D	One-Dimensional
3D	Three-Dimensional
CSDA	Continuous Slowing-Down Approximation
DDD	Displacement-Damage Dose
DSNE	Design Specification for Natural Environments
EM	Electromagnetic
ESA	European Space Agency
ETRAN	Electron TRANsport
FLUKA	Fluktuierende Kaskade
FMC	Forward Monte Carlo
GCR	Galactic-Cosmic Radiation
GRAS	Geant4 Radiation for Space
HLS	Human Launch System
HZETRN	High-*Z* and Energy Transport
ITS	Integrated Tiger Series
keV	Kilo-Electron-Volt
LET	Linear Energy Transfer
MCNP	Monte Carlo for N-Particles
MeV	Megaelectronvolt
MPCV	Multi-Program Crew Vehicle
MSFC	Marshall Space Flight Center
NESC	NASA Engineering and Safety Center
NIST	National Institute of Standards and Technology
PHITS	Particle and Heavy Ion Transport Code
PTFE	Polytetrafluoroethylene
RDM	Radiation Design Margin
RMC	Reverse Monte Carlo
SEE	Single Event Effects
SLS	Space Launch System
TID	Total Ionizing Dose
TIGER	Trans-Iron Galactic Element Recorder
µm	Micrometer

12.0 References

1. B. Jun, X. Zhu, L. Martinez-Sierra, I. Jun, "Inter-Comparison of Ionizing Doses from Space Shielding Analyses using MCNP, Geant4, FASTRAD, and NOVICE," *IEEE Transactions on Nuclear Science*, https://doi.org/10.1109/TNS.2020.2979657 (2020)
2. W. Kim, J. Z. Chinn, I. Katz, H. B. Garrett, K. F. Wong, "3-D NUMIT: A General 3-D Internal Charging Code," *IEEE Transactions on Plasma Science*, vol. 45, 2298, 2017.
3. R. Reed, R. A. Weller, A. Akkerman, J. Barak, W. Culpepper, et al., "Anthology of the development of radiation transport tools as applied to single event effects," *IEEE Transactions on Nuclear Science*, Vol. 60, pp. 1876-1911 (2013).
4. FASTRAD, A Radiation Analysis Software, by TRAD, Toulouse France, Available: http://www.trad.fr/FASTRADSoftware.html

5. Slaba TC, Wilson JW, Werneth CM, Whitman K. Updated deterministic radiation transport for future deep space missions. Life Sci Space Res (Amst). 2020 Nov;27:6-18. doi: 10.1016/j.lssr.2020.06.004. Epub 2020 Jun 17. PMID: 34756231.
6. J. W. Norbury, T. C. Slaba, N. Sobolevskyb, B. Redell, "Comparing HZETRN, SHIELD, FLUKA and GEANT transport codes," *Life Science in Space Research*, https://doi.org/10.1016/j.lssr.2017.04.001, Vol. 14, pp. 64-73, 2017
7. Geant4, (Geometry And Tracking), a platform for particle transport simulation using Monte Carlo methods. Available: https://geant4.web.cern.ch/
8. MCNP User's Manual Code Version 6.2, LA-UR-17-29981, 2017.
9. S. M. Seltzer, *Updated Calculations for Routine Space-Shielding Radiation Dose Estimates: SHIELDOSE-2*, Technical Report PB95-171039, National Institute of Standards and Technology, Gaithersburg, MD, December 1994.
10. T. W. L., Ronald. P. Kensek, B. C. Franke, M. J. Crawford, G. D. Valdez, "ITS version 6.4: The Integrated TIGER Series of Monte Carlo Electron/Photon Radiation Transport Codes," ANS RPSD 2014 - *18th Topical Meeting of the Radiation Protection & Shielding Division of ANS*, Knoxville, TN, September 14 – 18, 2014, American Nuclear Society, LaGrange Park, IL, 2014.
11. FLUKA. Available: http://www.fluka.org/fluka.php
12. T. M. Jordan, "NOVICE a Radiation Transport/Shielding Code," Experimental and Mathematical Physics Consultants, Rep.EMP.L82.001. 2982. Available: https://empc.com/
13. T. M. Jordan, "An adjoint charged particle transport method," *IEEE Trans. Nucl. Sci.*, vol. NS-23, no. 6, pp. 1857-1861, Dec. 1976.
14. L. Desorgher, F. Lei, G. Santin, "Implementation of the reverse/adjoint Monte Carlo method into Geant4," *Nuclear Instruments and Methods in Physics Research Section A: Accelerators, Spectrometers, Detectors and Associated Equipment*, Volume 621, Issues 1–3, 2010, Pages 247-257, ISSN 0168-9002, https://doi.org/10.1016/j.nima.2010.06.001.
15. G. Santin, V. Ivanchenko, H. Evans, P. Nieminen and E. Daly, "GRAS: a general-purpose 3-D Modular Simulation tool for space environment effects analysis," in *IEEE Transactions on Nuclear Science*, vol. 52, no. 6, pp. 2294-2299, Dec. 2005, doi: 10.1109/TNS.2005.860749. Available: https://essr.esa.int/project/gras-geant4-radiation-analysis-for-space.
16. P. Pourrouquet, A. Varotsou, L. Sarie, J-C. Thomas, N. Chatry, D. Standarovski, G. Rolland, and C. Barillot, "Comparative study between Monte-Carlo tools for space applications," Proc. *16th Eur. RADECS Conf.* paper number C1, Sep. 19-23, 2016.
17. I. Jun, S. Kang, G. Santin, and P. Nieminen, "Shielding Code Comparison: A Simple Benchmark Problem," *EJSM Instrument Workwhop*, Noordwijk, Netherlands, Jan 8-10, 2010.
18. G. Santin, S. Kamg, I.Jun, P. Nieminen, et al., "A radiation transport code benchmarking study for the EJSM mission," *IEEE Nuclear Science Symposium & Medical Imaging Conference*, 10.1109/NSSMIC.2010.5873852, Nov., 2010.
19. M. Cherng, I. Jun, and T. M. Jordan, "Optimum shielding in Jovian radiation environment," *Nucl. Instrum. Methods Phys. Res. Sec. A* 580, pp.633-636, 2007.
20. G. Martina, S. Christoph, W. Uli, R. Marta, S. Giovanni, W. N. John, T. Emanuele, M. Alessandra, B. Luca, L. Cesare, D. Marco, and T. Chiara La, "Accelerator-Based Tests of

Shielding Effectiveness of Different Materials and Multilayers using High-Energy Light and Heavy Ions," *Radiation Research*, vol. 190, no. 5, pp. 526-537, Aug. 2018.
21. T. C. Slaba, A. A. Bahadori, B. D. Reddell, R. C. Singleterry, M. S. Clowdsley, and S. R. Blattnig, "Optimal shielding thickness for galactic cosmic ray environments," *Life Sciences in Space Research*, vol. 12, pp. 1-15, Feb. 2017.
22. R. Mangeret, T. Carriere, J. Beaucour, and T. Jordan, "Effects of Material and/or Structure on Shielding of Electronic Devices," *IEEE Transactions on Plasma Science*, Vol. 43, No. 6, 1996.
23. S. Ibarmia, J. Eck, V. Ivanchenko, et al., "Experimental Dose Enhancement in Multi-Layer Shielding Structures Exposed to High-Energy Electron Environments," in *IEEE Transactions on Nuclear*, vol. 60, no. 4, pp. 2486-2493, Aug. 2013.
24. W. Atwell, K. Rojdev, S. Aghara, and S. Sriprisan, "Mitigating the Effects of the Space Radiation Environment: A Novel Approach of Using Graded-Z Materials," AIAA 2013-5385, https://doi.org/10.2514/6.2013-5385, Sept., 2013
25. I. Jun, "Effects of Secondary Particle on the Total Dose and the Displacement Damage in Space Proton Environments," *IEEE Transactions on Nuclear Science*, Vol. 48, No. 1, pp. 162-175 (2001).
26. I. Jun and W. McAlpine, "Displacement Damage in Silicon due to Secondary Neutrons, Pions, Deuterons, and Alphas from Proton Interactions with Materials," *IEEE Transactions on Nuclear Science*, Vol. 48, No. 6, pp. 2034-2038 (2001).
27. T. Armstrong and B/ Colborn, "Predictions of secondary neutrons and their importance to radiation effects inside the International Space Station," *Radiation Measurements*, Vol 33, pp. 229-234, 10.1016/s1350-4487(00)00152-9, 2001.
28. L. Heilbronn, T. Borak, L. Townsend, P. Tsai, C. Burnham, R. McBeth, "Neutron yields and effective doses produced by Galactic Cosmic Ray interactions in shielded environments in space," *Life Sciences in Space Research*, Vol., 7, pp. 90-99, https://doi.org/10.1016/j.lssr.2015.10.005, Nov, 2015.
29. C. Mertens, M. M. Meier, S. Brown, R. B. Norman, and X. Xu, "NAIRAS aircraft radiation model development, dose climatology, and initial validation," *Space Weather*, 11, 603–635, doi:10.1002/swe.20100,.2013.
30. I. Jun "Benchmark study for energy deposition by energetic electrons in thick elemental slabs: Monte Carlo results and experiments," *IEEE Trans. Nucl. Sci.*, vol. 50, no. 5, pp. 1732-1739, Oct. 2003.
31. G. A. Ruben, CERN, Personal Communication, 2020.
32. S. M. Seltzer, "Conversion of Depth-Dose Distributions from Slab to Spherical Geometries for Space-Shielding Applications," *IEEE Trans. Nucl. Sci.* NS-33, 1292 (1986).
33. S. M. Seltzer, "Electron-Photon Monte Carlo Calculations: The ETRAN Code," *Appl. Radiat. Isot.* 42, 917 (1991).
34. T. M. Jenkins, W.R. Nelson, and A. Rindi (editors) "Monte Carlo Transport of Electrons and Photons," *Ettore Majorana International Science Series*, Plenum (1988).
35. M. J. Berger, M. Inokuti, H. H. Andersen, H. Bichsel, J. A. Dennis, D. Powers, S. M. Seltzer, and J.E. Turner, *Stopping Powers for Electrons and Positrons*, Report 37 of the International Commission on Radiation Units and Measurements (1984).

36. R. Altstatt and D. Edwards, “Modeling natural space ionizing radiation effects on external materials,” Proc. *SPIE 4134, Photonics for Space Environments VII*, (26 October 2000); doi: 10.1117/12.405348.
37. S. M. Seltzer, “Calculation of Photon Mass Energy-Transfer and Mass Energy-Absorption Coefficients,” *Rad. Res.* 136, 147 (1993).
38. M. J. Berger, M. Inokuti, H. H. Andersen, H. Bichsel, D. Powers, S. M. Seltzer, D. Thwaites, and D. E. Watt, *Stopping Powers for Protons and Alpha Particles*, Report 49 of the International Commission on Radiation Units and Measurements (1993).
39. Cross-Program Design Specification for Natural Environment (DSNE), SLS-SPEC-159, Revision I, Effective Date: October 27, 2021.
40. W. K Stuckey and M.J. Meshishnek, *Solar Ultraviolet and Space Radiation Effects on Inflatable Materials*, Aerospace Report No. TR-2000(8565)-9, 2000.
41. Tatsuhiko Sato, Yosuke Iwamoto, Shintaro Hashimoto, Tatsuhiko Ogawa, Takuya Furuta, Shin-ichiro Abe, Takeshi Kai, Pi-En Tsai, Hunter N. Ratliff, Norihiro Matsuda, Hiroshi Iwase, Nobuhiro Shigyo, Lembit Sihver and Koji Niita “Features of Particle and Heavy Ion Transport code System (PHITS) version 3.02,” *J. Nucl. Sci. Technol.* 55, 684-690 (2018).

REPORT DOCUMENTATION PAGE

Form Approved
OMB No. 0704-0188

1. REPORT DATE *(DD-MM-YYYY)*	2. REPORT TYPE	3. DATES COVERED *(From - To)*
07/20/2023	Technical Memorandum	

4. TITLE AND SUBTITLE
Space-Shielding Radiation Dosage Code Evaluation
Phase 1: SHIELDOSE-2 Radiation-Assessment Code

5a. CONTRACT NUMBER

5b. GRANT NUMBER

5c. PROGRAM ELEMENT NUMBER

6. AUTHOR(S)
Gentz, Steven J.; Jun, Insoo

5d. PROJECT NUMBER

5e. TASK NUMBER

5f. WORK UNIT NUMBER
869021.01.23.01.01

7. PERFORMING ORGANIZATION NAME(S) AND ADDRESS(ES)
NASA Langley Research Center
Hampton, VA 23681-2199

8. PERFORMING ORGANIZATION REPORT NUMBER
NESC-RP-21-01718

9. SPONSORING/MONITORING AGENCY NAME(S) AND ADDRESS(ES)
National Aeronautics and Space Administration
Washington, DC 20546-0001

10. SPONSOR/MONITOR'S ACRONYM(S)
NASA

11. SPONSOR/MONITOR'S REPORT NUMBER(S)
NASA/TM-20230010640

12. DISTRIBUTION/AVAILABILITY STATEMENT
Unclassified - Unlimited
Subject Category
Availability: NASA STI Program (757) 864-9658

13. SUPPLEMENTARY NOTES

14. ABSTRACT
Radiation-transport codes or radiation-analysis tools are used in the spacecraft-design community to define and assess the local radiation levels. Among various radiation-transport/analysis tools available, SHIELDOSE-2 is commonly used in the early spacecraft-design phases because it has been established that it provides reasonably reliable results with relatively rapid computation time. The NASA Engineering and Safety Center initiated a two-phased study: (1) to better understand and document the SHIELDOSE-2 code capabilities and limitations, and (2) to recommend alternative tools to use for cases where SHIELDOSE-2 is not applicable. This report provides a summary of the Phase 1 study.

15. SUBJECT TERMS
SHIELDOSE-2; NASA Engineering and Safety Center; Radiation-Analysis Tools; Radiation-Transport Codes

16. SECURITY CLASSIFICATION OF:			17. LIMITATION OF ABSTRACT	18. NUMBER OF PAGES	19a. NAME OF RESPONSIBLE PERSON
a. REPORT	b. ABSTRACT	c. THIS PAGE			STI Help Desk (email: help@sti.nasa.gov)
U	U	U	UU	38	19b. TELEPHONE NUMBER *(Include area code)* (443) 757-5802